STArt
Sports Traumatology & Arthroscopy
DOI: 10.14744/STA.2025.71600
Sports Traumatol Arthrosc 2025;2(3):109–118

Original Article

Does Trochlear Dysplasia Affect Fluoroscopic Femoral Tunnel Placement During ACL Reconstruction?

Firat Dogruoz,[1] Yusuf Cakir,[1] Huseyin Kursat Celik[2]

[1]Department of Orthopedics and Traumatology, University of Health Sciences, Antalya Training and Research Hospital, Antalya, Türkiye
[2]Department of Agricultural Machinery and Technology Engineering, Akdeniz University, Antalya, Türkiye

ABSTRACT

Objective: Precise anatomical placement of the femoral tunnel is critical for successful outcomes in anterior cruciate ligament (ACL) reconstruction. Intraoperative fluoroscopic guidance is widely employed to improve tunnel accuracy, particularly using the Bernard–Hertel quadrant method on true lateral views. However, the influence of trochlear dysplasia, commonly seen in patients with patellofemoral instability, on the radiographic identification of the ACL femoral footprint remains unclear. Using the quadrant method, this study evaluated whether trochlear dysplasia affects fluoroscopic localization of the ACL femoral footprint.

Materials and Methods: 43 3D-printed femoral models were created from CT scans of patients with (n=21) and without (n=22) trochlear dysplasia. A consensus panel identified the anatomical ACL femoral footprint and marked it with a radiopaque thumbtack. True lateral fluoroscopic images were obtained under standardized conditions. Two independent observers performed radiographic measurements of the ACL footprint location using the ACL-X mobile application, applying the quadrant method. Intra- and inter-observer reliability was assessed using intraclass correlation coefficients (ICC). Group comparisons were made for the depth and height coordinates of the footprint.

Results: Radiographic measurements demonstrated excellent intra-observer reliability (ICC range: 0.854–0.912) and inter-observer (ICC range: 0.817–0.913). There was no significant difference in ACL footprint location between groups. The mean depth was 22.6±4.1% in the dysplasia group and 21.4±3.8% in the control group (p=0.807). Similarly, the mean height was 37.8±6.3% in the dysplasia group and 39.3±5.4% in controls (p=0.617). These findings indicate that trochlear dysplasia does not significantly affect radiographic footprint localization.

Conclusion: Trochlear dysplasia does not compromise the accuracy of fluoroscopic identification of the ACL femoral footprint using the quadrant method. Intraoperative fluoroscopic guidance remains reliable for anatomical femoral tunnel placement in ACL reconstruction, regardless of underlying trochlear morphology.

Keywords: Anterior cruciate ligament reconstruction, femoral tunnel placement, fluoroscopy, quadrant method, trochlear dysplasia

Cite this article as:
Dogruoz F, Cakir Y, Celik HK. Does Trochlear Dysplasia Affect Fluoroscopic Femoral Tunnel Placement During ACL Reconstruction?. Sports Traumatol Arthrosc 2025;2(3):109–118.

Address for correspondence:
Yusuf Cakir.
Department of Orthopedics and Traumatology, University of Health Sciences, Antalya Training and Research Hospital, Antalya, Türkiye
E-mail:
yusufcakir993@gmail.com

Submitted: 30.09.2025
Revised: 15.10.2025
Accepted: 21.10.2025
Available Online: 22.12.2025

Sports Traumatology & Arthroscopy – Available online at www.stajournal.com

INTRODUCTION

Anterior cruciate ligament (ACL) reconstruction is a standard orthopedic procedure to restore knee stability and function after ACL injury. Successful outcomes in ACL reconstruction are highly dependent on precise anatomical placement of the femoral tunnel, as incorrect positioning can lead to graft failure, persistent instability, and impaired knee kinematics [1,2]. During surgery, anatomical landmarks such as the intercondylar ridge and bifurcate ridge, along with remnant fibers, serve as essential guides for identifying the native femoral attachment site of the ACL [3]. In addition to these anatomical references, fluoroscopic techniques, particularly the quadrant method described by Bernard et al., have been widely adopted intraoperatively to guide femoral tunnel placement [4,5]. This method utilizes a true lateral radiographic view, enabling precise localization of the anatomical ACL femoral footprint.

Recent studies comparing femoral tunnel placement techniques have further supported the use of intraoperative fluoroscopy. Dong et al. demonstrated that combining fluoroscopy with anatomical measurements based on the apex of deep cartilage significantly improved the accuracy of femoral tunnel positioning and led to superior postoperative knee function and stability compared to the traditional bony landmark method [6]. Similarly, another study found that fluoroscopic guidance, particularly when using the quadrant method on a true lateral radiographic view, reduced tunnel placement errors and provided better alignment with the native ACL footprint [7]. These findings underscore the clinical value of fluoroscopy-assisted techniques, especially for ensuring consistent and anatomically accurate tunnel positioning during ACL reconstruction.

Although ACL injuries and patellofemoral instability (PFI) are traditionally viewed as separate conditions, recent evidence indicates that they may coexist, particularly in young and active individuals. Both injuries often result from similar non-contact mechanisms, suggesting a shared biomechanical predisposition [8–10]. Epidemiological studies have reported notable rates of simultaneous occurrence, reinforcing the importance of recognizing coexisting PFI during ACL injury assessment [11,12].

Importantly, the morphology of the distal femur—especially the trochlear region—can affect how anatomical landmarks appear on lateral fluoroscopic images [13]. Trochlear dysplasia, which is common in patients with PFI, may distort these landmarks and complicate accurate femoral tunnel placement [14]. Despite its relevance, the influence of trochlear morphology on fluoroscopic localization of the ACL femoral footprint remains underexplored.

The quadrant method is widely used; however, its reliability may be compromised in patients with abnormal distal femoral anatomy. Variations such as trochlear dysplasia can lead to misinterpretation of fluoroscopic landmarks, potentially resulting in femoral tunnel malposition. This study investigates whether trochlear morphology affects the accuracy of ACL femoral footprint localization using fluoroscopy.

Using three-dimensional (3D) printed femur models from patients with and without trochlear dysplasia, we evaluated how trochlear shape influences fluoroscopic localization of the ACL footprint via the quadrant method.

We hypothesized that trochlear dysplasia may significantly influence fluoroscopic interpretation, potentially causing deviations from the true anatomical position of the ACL femoral footprint.

MATERIALS AND METHODS

Patient Selection and Study Protocol

This experimental research utilized 3D-printed femoral models to evaluate the accuracy of the fluoroscopic identification of the ACL femoral footprint using the Bernard–Hertel quadrant method in knees with and without trochlear dysplasia. A retrospective review of radiological data was carried out using our institutional digital archive, encompassing patients treated for patellar instability between 2015 and 2024. From the identified 204 cases, a random sample was selected from those who had undergone CT imaging. For the control group, patients who presented to the emergency department with acute knee trauma and received CT imaging due to suspected fractures were screened. Individuals showing radiological features of trochlear dysplasia were excluded. Subjects with a prior history of knee surgery, fractures, congenital anomalies, or deformities, as well as those with suboptimal CT quality unsuitable for 3D reconstruction, were not included in the final analysis for either group. Institutional Review Board approval was secured before initiating the study (Approval Date/ID: 2025/9-4). The study adhered to the ethical standards outlined in the Declaration of Helsinki and its later revisions.

Sample Size Calculation

The sample size for this study was determined using G*Power software (version 3.1.9.7), assuming equal group allocation [15]. The calculation was based on a two-tailed independent t-test with an effect size (Cohen's d) of 1.0, derived from prior data reporting a standard deviation of 2.5% in the radiographic localization of the ACL femoral footprint using the Bernard–Hertel quadrant method [4,5]. To detect a clinically relevant difference of 2.5% between knees with and without trochlear dysplasia, with 80% power ($1 - \beta = 0.80$) and a significance level of $\alpha = 0.05$, the analysis indicated that a minimum of 34 knees (17 per group) would be required. To account for potential exclusions due to poor image quality, inadequate lateral fluoroscopic projections, or technically unusable CT data for

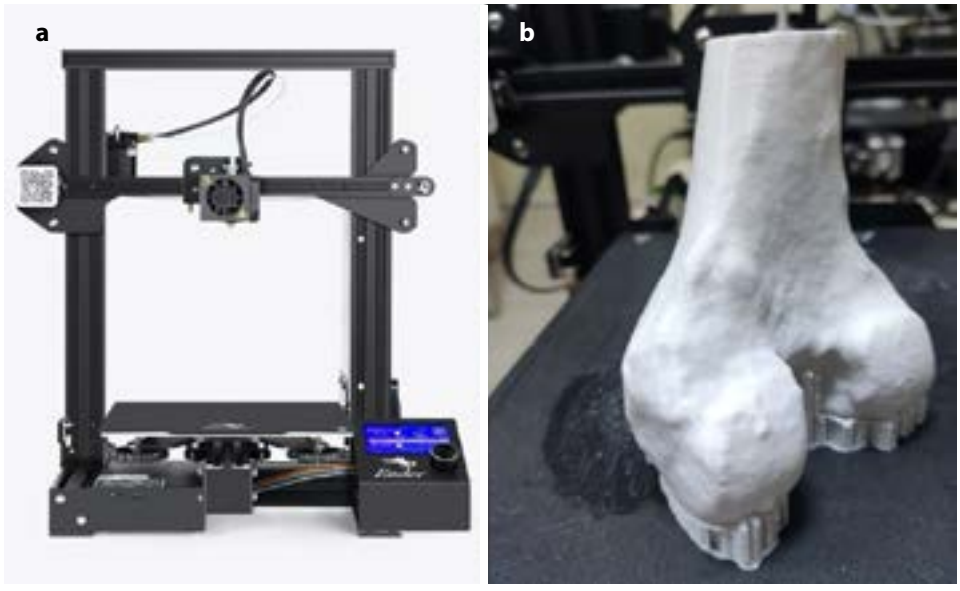

Figure 1. (a) The Creality Ender-3 Pro 3D printer manufacturing the femoral models. **(b)** A representative 3D-printed distal femur model generated from CT data demonstrates anatomical accuracy suitable for fluoroscopic ACL femoral footprint localization evaluation.

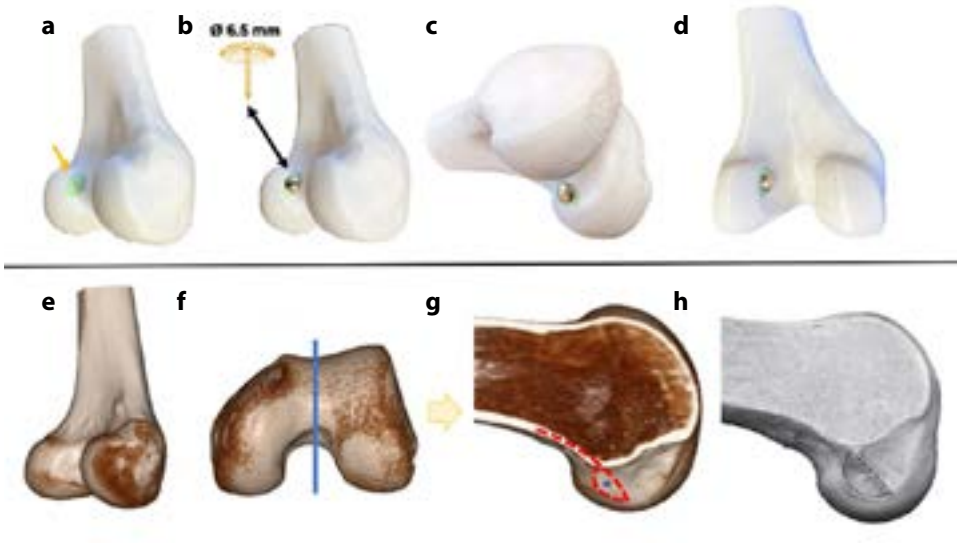

Figure 2. (a-d) Placement of a 6.5 mm diameter radiopaque metallic marker on the anatomically defined center of the ACL femoral footprint on 3D-printed distal femur models, as determined by expert consensus using CT data and anatomical landmarks (yellow arrow indicates the footprint region). **(e-g)** Digital visualization of the ACL footprint using multiplanar CT reconstruction. **(f)** Coronal plane reference line; **(g)** sagittal cross-section showing the anatomical location of the ACL footprint (dashed red outline) on the posteromedial surface of the lateral femoral condyle. **(h)** Comparative anatomical reference image illustrating the native femoral footprint of the ACL in a cadaveric specimen.

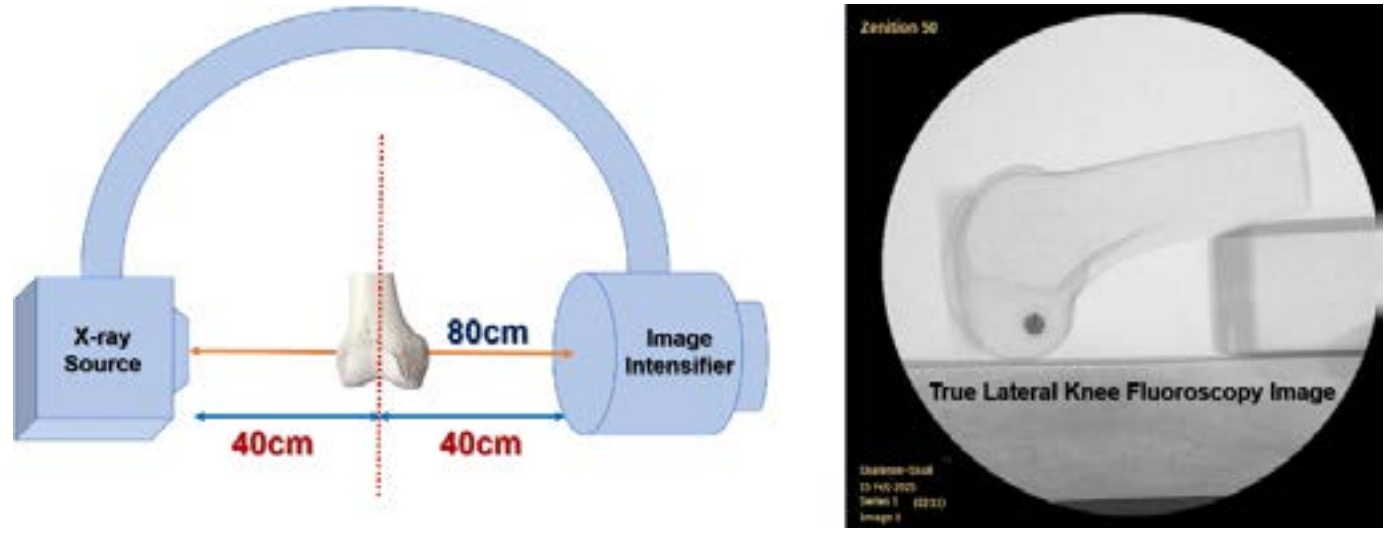

Figure 3. Fluoroscopic imaging setup and representative true lateral radiograph of a 3D-printed femoral model. The model was positioned equidistantly between the X-ray source and image intensifier of a C-arm system, with lateral beam orientation and adjustment to achieve perfect superimposition of the posterior femoral condyles. This positioning ensured an anatomically accurate lateral projection for analysis of ACL femoral footprint localization.

3D reconstruction, additional patients were initially screened to ensure a sufficient number of valid cases could be analyzed.

Three-Dimensional Model Production

CT scans were obtained for all participants using the CT unit (Siemens go. up, Siemens, Munich, Germany) located in either the Radiology or Emergency Department. The imaging protocol included a tube voltage of 121 kV (range: 120–130 kV), a tube current of 143 mA (range: 61–200 mA), a slice thickness of 0.6 mm (range: 0.2–0.8 mm), and a field of view (FoV) of 200 mm (range: 147–269 mm). Using the acquired DICOM data, three-dimensional digital models of the femur were reconstructed using Materialise Mimics and 3-Matic Medical software (Materialise NV, Leuven, Belgium). The STL files were processed using Ultimaker Cura (Ultimaker B.V., Netherlands) and printed with a Creality Ender-3 Pro 3D printer (Shenzhen, China) as shown in Figure 1. The printing settings were configured with an infill density of 3–10% and a layer height of 0.16–0.20 mm to achieve an optimal balance between model durability and anatomical fidelity. Polylactic acid (PLA) filament was selected for its cost-effectiveness and ability to produce dimensionally accurate, robust models suitable for handling and fluoroscopic assessment. Following fabrication, each printed model was visually and digitally compared with the original 3D CT reconstruction to verify the accurate representation of key anatomical landmarks, especially those relevant to identifying the femoral footprint of the ACL. This validation step ensured the reliability of the models for subsequent fluoroscopic analysis.

Determination of the ACL Femoral Footprint on Printed Models

The precise anatomical location of the femoral footprint of the anterior cruciate ligament (ACL) was identified through a consensus by a panel composed of two orthopedic surgeons with over ten years of experience in knee surgery and sports traumatology and one anatomist. To improve accuracy and reduce the risk of localization error, the panel evaluated each case using both the patients' original CT images and their corresponding 3D-printed femoral models simultaneously. Anatomically, the ACL femoral footprint is located on the posteromedial surface of the lateral femoral condyle, situated within the intercondylar notch, posterior to the lateral intercondylar ridge (Resident's ridge), and anterior and superior to the lateral bifurcate ridge, which separates the native insertion sites of the ACL's anteromedial and posterolateral bundles. Once the center of the footprint was identified, a metallic thumbtack with a head diameter of 6.5 mm was securely fixed to this point on each model. This radiopaque marker enabled clear and consistent visualization of the anatomical ACL footprint on fluoroscopic images (Fig. 2)

Fluoroscopy Technique and Image Acquisition

Fluoroscopic evaluations were performed in an operating room environment using a C-arm system (Zenition 50, Philips, The Netherlands). The 3D-printed femoral models were positioned equidistantly between the X-ray source and the image intensifier during image acquisition. Care was taken to align the deepest point of the trochlear groove precisely at the midpoint between

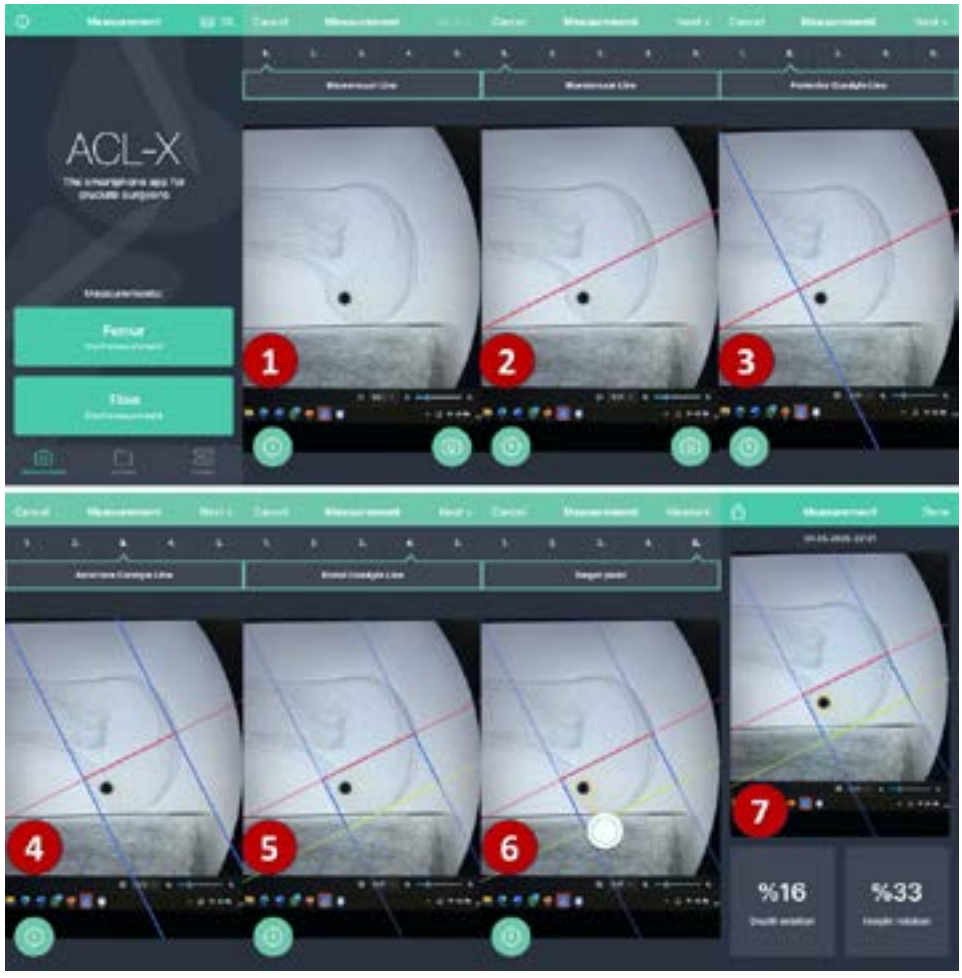

Figure 4. Measurement of the ACL femoral footprint location using the quadrant method on true lateral fluoroscopic imaging via the ACL-X mobile application. (Image 1): A true lateral fluoroscopic image of the femur is obtained with optimal superimposition of the posterior femoral condyles. A radiopaque marker (black circle) represents the center of the anatomically defined ACL femoral footprint. (Image 2): The Blumensaat line (roof of the intercondylar notch) is drawn (red line), forming the horizontal reference axis. (Image 3): A perpendicular line is drawn from the posterior cortical margin of the lateral femoral condyle to the Blumensaat line, representing the posterior border (blue line). (Image 4): The anterior and posterior borders of the lateral femoral condyle are marked to define the sagittal width of the condyle. (Image 5): Superior (Blumensaat) and inferior (distal condyle) borders of the condyle are marked, forming a grid over the lateral condyle. (Image 6): The center of the metal marker (ACL footprint) is selected as the target point. The application calculates its position within the grid. (Image 7): The final screen displays the depth and height ratio of the ACL footprint center within the quadrant, given as percentages: 16% from the posterior cortex (depth) and 33% from the Blumensaat line (height), indicating a typical anatomical location.

the medial and lateral cortical outlines. The X-ray source was placed on the lateral side of the specimen to simulate standard lateral knee imaging. Image acquisition parameters included a tube voltage ranging from 45 to 52 kV and a tube current between 0.4 and 1.8 mA. Each model was carefully rotated until the posterior margins of the medial and lateral femoral condyles

Table 1. Comparison of demographic and clinical characteristics of patients

Variables	Trochlear Dysplasia Group (n=21)	Control Group (n=22)	p
Age (years ±SD)	22.1±7.4	24.8±8.1	0.263[1]
Sex (n, %)			0.219[2]
Male	8 (38.1%)	12 (54.5%)	
Female	13 (61.9%)	10 (45.5%)	
Side (n, %)			0.137[2]
Right	7 (33.3%)	12 (54.5%)	
Left	14 (66.7%)	10 (45.5%)	
Weight (kg ±SD)	70.1±17.5	76.3±13.1	0.593[3]
Height (cm ±SD)	168.3±12.1	173.0±8.6	0.148[3]
BMI (kg/m2±SD)	24.5±4.8	25.3±4.8	0.556[1]
TT-TG Distance (mm ±SD)	22.7±4.1	13.1±3.4	0.001[3]
TT-PCL Distance (mm ±SD)	17.9±4.3	11.4±4.5	0.001[3]
Dejour Classification (n, %)			NA
Type A	5 (23.8%)	-	
Type B	7 (33.3%)	-	
Type C	4 (19.0%)	-	
Type D	5 (23.8%)	-	
Caton-Deschamps Index	1.09±0.15	0.88±0.11	0.001[3]
Patellar Tilt (°±SD)	32.5±11.2	9.5±4.7	0.001[3]
Tibiofemoral rotation (°±SD)	8.9±4.1	5.6±3.6	0.008[1]

were perfectly superimposed to obtain an anatomically accurate true lateral projection. 5 to 10 images were captured for each femur, and the most accurate lateral projection, demonstrating ideal condylar overlap, was selected for analysis. Figure 3 shows the fluoroscopic imaging setup and a representative image

Radiological Measurements on Digital Fluoroscopic Images

Radiological measurements were performed using the ACL-X smartphone application (Linova Software GmbH, v.1.0.2, Munich, Germany), a dedicated mobile software developed to accurately assess cruciate ligament footprint localization on lateral fluoroscopic images [16,17]. The application enables the standardized application of the quadrant method and provides automated calculation of the depth and height ratios of the ACL femoral footprint. Two independent observers, one musculoskeletal radiologist and one orthopedic surgeon specializing in sports traumatology, individually conducted the measurements on the smartphone interface. All images were evaluated in a randomized sequence to prevent order bias. Each observer repeated the entire assessment process on a separate occasion, with a minimum interval of two weeks between the two measurement rounds, allowing for an analysis of intra-observer reliability. To minimize recall bias, the observers were blinded to their prior measurements and those of the other observer. The ACL-X mobile app was used to calculate the final measurements of the ACL femoral footprint location with the quadrant method, as demonstrated in Figure 4.

Inter- and intra-observer reliability of the measurements was tested using an interclass correlation coefficient (ICC). The ICC was above 0.800 (acceptable reliability) for all variables, and the mean of the measurements was employed for the final analysis.

Statistical Analysis

Continuous variables were described using the mean, standard deviation, and range, while categorical data were expressed as frequencies and percentages. The Kolmogorov-Smirnov test was used to determine whether continuous variables conformed to a normal distribution. For data that follows a normal distribution, parametric tests were applied; non-parametric tests were used for data that does not adhere to this distribution. The

Table 2. Inter- and intra-observer reliability results

Variables	Intra-observer Reliability (ICC, 95% CI)		Interobserver Reliability (ICC, 95% CI)	
	A t1 vs. A t2	B t1 vs. B t2	A t1 vs. B t1	A t2 vs. B t2
ACL Depth	0.910 (0.841-0.950)	0.912 (0.844-0.952)	0.913 (0.846-0.952)	0.908 (0.836-0.949)
ACL Height	0.854 (0.747-0.918)	0.817 (0.814-0.945)	0.817 (0.661-0.901)	0.901 (0.816-0.946)

Table 3. Comparison of the center of the ACL femoral footprint between groups

Variables	Trochlear Dysplasia Group	Control Group	Total	p
ACL Depth (%)	22.6±4.14	21.4±3.83	22.0±3.98	0.807
ACL Height (%)	37.8±6.30	39.3±5.40	38.6±5.83	0.617

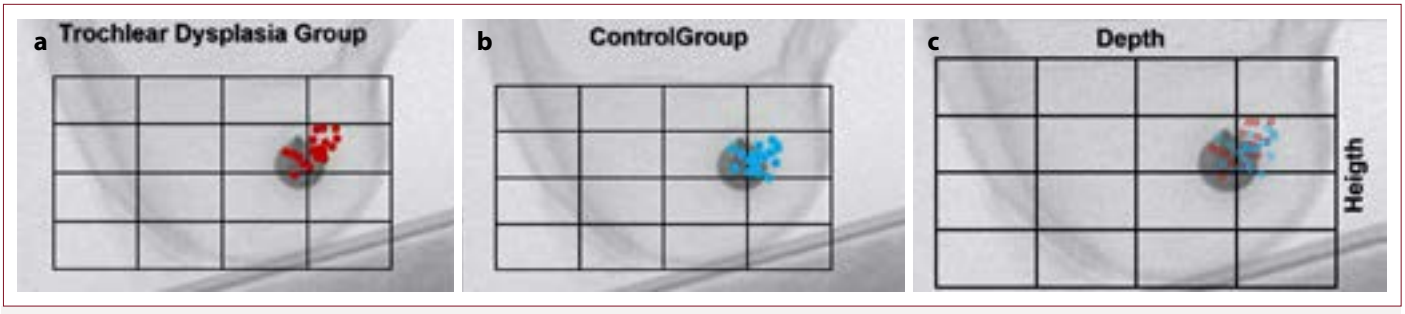

Figure 5. Distribution of ACL femoral footprint coordinates according to the quadrant method. **(a)** Scatterplot of depth and height coordinates in the Trochlear Dysplasia group (red dots), **(b)** Scatterplot of coordinates in the Control group (blue dots), **(c)** Superimposed view showing both groups for comparison (red = dysplasia, blue = control). All measurements were mapped on standardized quadrant reference images derived from true lateral fluoroscopic views. The center of each plotted point represents the radiologically determined ACL footprint location as a percentage of the lateral femoral condyle's total depth (horizontal axis) and height (vertical axis).

independent sample t-test or the Mann-Whitney U test was used to compare continuous variables, while the chi-squared test was employed to compare categorical data. Intra-observer and inter-observer reliability were evaluated using Intraclass Correlation Coefficients (ICC) with 95% confidence intervals (CIs). A two-way random-effects model was used to assess interobserver reliability, considering both absolute agreement and consistency. ICC values were interpreted as poor (<0.50), moderate (0.50–0.75), good (0.75–0.90), or excellent (>0.90) [18]. A p-value of less than 0.05 was deemed statistically significant.

RESULTS

Demographic and Radiological Characteristics

A total of 43 femoral models were evaluated, including 21 models in the trochlear dysplasia group and 22 in the control group. The mean age was 22.1±7.4 years in the dysplasia group and 24.8±8.1 years in the control group, with no statistically significant difference (p=0.263). The distribution of sex and laterality was similar between groups (p=0.219 and p=0.137, respectively). Anthropometric parameters such as body weight, height, and BMI were also comparable (p>0.05 for all). Radiological comparisons revealed significantly greater mean TT-TG (22.7±4.1 mm vs. 13.1±3.4 mm, p=0.001), TT-PCL (17.9±4.3 mm vs. 11.4±4.5 mm, p=0.001), and Caton-Deschamps index values (1.09±0.15 vs. 0.88±0.11, p=0.001) in the dysplasia group compared to controls. Additionally, the dysplasia group demonstrated significantly higher patellar tilt angles (32.5°±11.2° vs. 9.5°±4.7°, p=0.001) and tibiofemoral rotation (8.9°±4.1° vs. 5.6°±3.6°, p=0.008) (Table 1).

Reliability of Measurements

Intra-observer reliability for ACL footprint depth and height

measurements showed excellent consistency, with intraclass correlation coefficients (ICC) ranging from 0.854 to 0.912. Interobserver agreement was also high, with ICC values ranging from 0.817 to 0.913 (Table 2).

Comparison of ACL Footprint Location Between Groups

The position of the ACL femoral footprint, expressed as a percentage relative to the quadrant method, did not differ significantly between groups. The mean depth was 22.6±4.1% in the dysplasia group and 21.4±3.8% in the control group (p=0.807), while the mean height was 37.8±6.3% and 39.3±5.4%, respectively (p=0.617) (Table 3). These results suggest that the anatomical ACL footprint location remains consistent, independent of trochlear morphology (Fig. 5).

DISCUSSION

The principal finding of this study is that trochlear dysplasia does not significantly alter the radiographic localization of the ACL femoral footprint when using the quadrant method on true lateral fluoroscopic images. Despite marked anatomical differences in distal femoral morphology and radiographic parameters between the dysplasia and control groups, the depth and height coordinates of the femoral footprint remained statistically comparable. This suggests that the quadrant method provides a reliable reference for femoral tunnel placement during ACL reconstruction, even in the presence of trochlear morphological variations, often associated with patellofemoral instability. These findings support the continued use of fluoroscopic guidance as a reproducible intraoperative tool, highlighting that trochlear dysplasia alone may not necessitate deviation from standard anatomical tunnel placement techniques.

Numerous cadaveric and radiologic studies have sought to define the center of this footprint using the Bernard-Hertel quadrant method. Still, reported coordinates have shown considerable variability, raising concerns about the method's generalizability and reproducibility across populations and imaging modalities [19,20]. In the current study, the mean location of the ACL femoral footprint was measured at 22.6% (depth) and 37.8% (height) in the trochlear dysplasia group, and at 21.4% and 39.3%, respectively, in the control group. These findings are consistent with—but slightly more anterior than—the original values proposed by Bernard et al., who described the anatomical center of the ACL footprint at 24.8% (deep–shallow) and 28.5% (high–low) using the quadrant method on lateral radiographs of cadaveric knees [4,5]. In the extensive cadaveric review by Parkar et al., the weighted mean center of the ACL femoral footprint was 29% (depth) and 35% (height), with a 5th–95th percentile range of 24–37% and 28–43%, respectively [19]. The control group's footprint location fell slightly anterior to this range, particularly in depth, suggesting population-specific variation or methodological differences in 3D model positioning and fluoroscopic imaging. Xu et al. synthesized results from 13 studies and reported a pooled footprint location at 28.4% ± 5.1% (depth) and 35.7% ± 6.9% (height), defining a "standard area" centered at 27.53% and 35.85% [21]. In our study, some values, particularly from the trochlear dysplasia group, fell outside this standard area, although the differences were not statistically significant. These findings suggest that while the Bernard quadrant method remains valid, trochlear morphology may introduce subtle variation in radiographic footprint interpretation, reinforcing the need for careful intraoperative assessment in dysplastic knees.

While this study primarily focused on the impact of trochlear morphology, previous literature has also emphasized the clinical relevance of addressing concurrent patellofemoral instability (PFI) in ACL-injured patients. Several studies have suggested that untreated PFI may negatively affect surgical outcomes, particularly when MPFL injury is present. Our findings complement these reports by demonstrating that, even in the presence of dysplastic trochlear anatomy, reliable femoral tunnel placement can still be achieved using fluoroscopic guidance.

The strengths of the current study include the use of standardized 3D-printed femoral models derived from high-resolution CT scans, precise control of fluoroscopic conditions, and a validated digital measurement application (ACL-X) that enhances reproducibility. Observer blinding, repeated measurements, and excellent inter/intra-observer reliability further strengthen the methodological rigor. However, several limitations should be acknowledged. First, static bone models may not fully replicate intraoperative variables such as soft tissue interference, surgical positioning, or fluoroscopic limitations in live patients. Second, although true lateral projections were carefully selected, slight deviations from ideal positioning in clinical practice could affect measurement accuracy. Finally, this was a cadaveric model-based study with a relatively limited sample size, and larger clinical validation is warranted before generalizing the results to all surgical scenarios

In conclusion, this experimental study demonstrates that trochlear dysplasia does not significantly affect the fluoroscopic localization of the ACL femoral footprint when using the Bernard–Hertel quadrant method. Despite anatomical variations associated with dysplasia, the depth and height coordinates of the ACL footprint remained consistent between dysplastic and non-dysplastic femurs. These findings confirm the reliability of intraoperative fluoroscopic guidance for femoral tunnel placement, even in the presence of altered

distal femoral morphology. From a surgical perspective, this supports the continued use of the quadrant method as a standardized approach for anatomic ACL reconstruction without the need for significant adjustments in patients with trochlear dysplasia. Clinically, the routine application of this method may improve tunnel accuracy and reduce the risk of graft malposition, especially when traditional bony landmarks are obscured or distorted. Future clinical studies involving intraoperative data and postoperative outcomes are warranted to validate these findings in real-world surgical scenarios and to explore whether subtle radiographic deviations may influence long-term graft function or failure rates.

DECLARATIONS

Ethics Committee Approval: Antalya Training and Research Hospital Ethics Committee approved this study (Date: 29/05/2025, Number: 9-4).

Informed Consent: Informed consent was not deemed necessary for this study.

Conflict of Interest: The authors declared they have no conflicts of interest.

Financial Disclosure: The authors declared that they have no relevant or material financial interests that relate to the research described in this paper.

Funding Disclosure: No funding was received for this study.

Data Avaliability Statement: Data are available from the corresponding author upon reasonable request.

Use of AI for Writing Assistance: The authors declared that they did not use any generative artificial intelligence for the writing of this manuscript, nor for the creation of images, graphics, tables, or their corresponding captions.

Author Contributions: Concept – FD, HKC, YC; Design – FD, HKC, YC; Supervision – FD, HKC, YC; Data collection and/or processing – FD, YC; Analysis and/or interpretation – FD, HKC; Literature search – FD, HKC, YC; Writing – FD, HKC, YC; Critical review – HKC; References and fundings – FD, HKC, YC.

Peer-review: Externally peer-reviewed.

ABBREVIATIONS

ACL – Anterior Cruciate Ligament

ACL-X – ACL Localization Mobile Application

BMI – Body Mass Index

CI – Confidence Interval

CT – Computed Tomography

DICOM – Digital Imaging and Communications in Medicine

FoV – Field of View

ICC – Intraclass Correlation Coefficient

kVp – Kilovolt Peak

mA – Milliampere

MPFL – Medial patellofemoral ligament

PFI – Patellofemoral Instability

PLA – Polylactic Acid

TT-PCL – Tibial Tubercle–Posterior Cruciate Ligament distance

TT-TG – Tibial Tubercle–Trochlear Groove distance

REFERENCES

1. Byrne KJ, Hughes JD, Gibbs C, Vaswani R, Meredith SJ, Popchak A, et al. Non-anatomic tunnel position increases the risk of revision anterior cruciate ligament reconstruction. Knee Surg Sports Traumatol Arthrosc 2022;30:1388-95. [Crossref]
2. Lim HC, Yoon YC, Wang JH, Bae JH. Anatomical versus non-anatomical single bundle anterior cruciate ligament reconstruction: a cadaveric study of comparison of knee stability. Clin Orthop Surg 2012;4:249-55. [Crossref]
3. Ferretti M, Ekdahl M, Shen W, Fu FH. Osseous landmarks of the femoral attachment of the anterior cruciate ligament: an anatomic study. Arthroscopy 2007;23:1218-25. [Crossref]
4. Bernard M, Hertel P. Intraoperative and postoperative insertion control of anterior cruciate ligament-plasty. A radiologic measuring method (quadrant method). Unfallchirurg 1996;99:332-40. [Article in German]
5. Bernard M, Hertel P, Hornung H, Cierpinski T. Femoral insertion of the ACL. Radiographic quadrant method. Am J Knee Surg 1997;10:14-21;discussion 21-2.
6. Dong Y, Gao Y, Cui P, He Y, Yao G. Comparison of femoral tunnel position and knee function in anterior cruciate ligament reconstruction: a retrospective cohort study using measuring-fluoroscopy method versus bony marker method. BMC Musculoskelet Disord 2024;25:572. [Crossref]
7. Inderhaug E, Larsen A, Waaler PA, Strand T, Harlem T, Solheim E. The effect of intraoperative fluoroscopy on the accuracy of femoral tunnel placement in single-bundle anatomic ACL reconstruction. Knee Surg Sports Traumatol Arthrosc 2017;25:1211-8. [Crossref]
8. Macura M, Veselko M. Simultaneous reconstruction of ruptured anterior cruciate ligament and medial patellofemoral ligament with ipsilateral quadriceps grafts. Arthroscopy 2010;26:1258-62. [Crossref]
9. Hiemstra LA, Kerslake S, Heard M, Buchko G, Lafave M. Outcomes of surgical stabilization in patients with combined ACL deficiency and patellofemoral instability - A case series. Knee 2016;23:1106-11. [Crossref]
10. Shankar V, Natiq Hussain S, Sahanand S, Rajan D. Concurrent Anterior Cruciate Ligament and Medial Patellofemoral Ligament Reconstruction: A Case Report and Literature Review. Cureus 2020;12:e7717. [Crossref]

11. Sillanpaa PJ, Maenpaa H, Elo J, Mattila VM, Pihlajamaki H: Paper 139: incidence and nature of simultaneous anterior cruciate ligament injury and patellar dislocation-analysis of 130 708 young adults. Arthroscopy. 2012;28:e417-8. [Crossref]
12. Wu X, Chen J, Ye Z, Dong S, Xie G, Zhao S, Xu C, Li Z, Xu J, Zhao J. Clinical and Radiological Outcomes After Combined ACL and MPFL Reconstruction Versus Isolated ACL Reconstruction for ACL Injury With Patellar Instability. Am J Sports Med 2024;52:936-47. [Crossref]
13. Izadpanah K, Meine H, Kubosch J, Lang G, Fuchs A, Maier D, Ogon P, Südkamp NP, Feucht MJ. Fluoroscopic guided tunnel placement during medial patellofemoral ligament reconstruction is not accurate in patients with severe trochlear dysplasia. Knee Surg Sports Traumatol Arthrosc 2020;28:759-66. [Crossref]
14. Sanchis-Alfonso V, Ramírez-Fuentes C, Montesinos-Berry E, Elía I, Martí-Bonmatí L. Radiographic Location Does Not Ensure a Precise Anatomic Location of the Femoral Fixation Site in Medial Patellofemoral Ligament Reconstruction. Orthop J Sports Med 2017;5:2325967117739252. [Crossref]
15. Faul F, Erdfelder E, Lang AG, Buchner A. G*Power 3: a flexible statistical power analysis program for the social, behavioral, and biomedical sciences. Behav Res Methods. 2007;39:175-91. [Crossref]
16. Mueller MM, Tenfelde O, Hinz N, Pagenstert G, Frosch KH, Hoeher J, Akoto R. App-based analysis of the femoral tunnel position in ACL reconstruction using the quadrant method. Arch Orthop Trauma Surg 2024;144:3137-44. [Crossref]
17. Hoeher J, Tenfelde O, Wagener B, Fink M, Mauri-Moeller A, Balke M. App-Based Analysis of Fluoroscopic Images According to Bernard-Hertel Method for the Determination of Femoral Tunnel Positioning in Anterior Cruciate Ligament Reconstruction. Arthrosc Tech 2024;13:102863. [Crossref]
18. Koo TK, Li MY. A Guideline of Selecting and Reporting Intraclass Correlation Coefficients for Reliability Research. J Chiropr Med 2016;15:155-63. [Crossref]
19. Bird JH, Carmont MR, Dhillon M, Smith N, Brown C, Thompson P, Spalding T. Validation of a new technique to determine midbundle femoral tunnel position in anterior cruciate ligament reconstruction using 3-dimensional computed tomography analysis. Arthroscopy 2011;27:1259-67. [Crossref]
20. Parkar AP, Adriaensen MEAPM, Vindfeld S, Solheim E. The Anatomic Centers of the Femoral and Tibial Insertions of the Anterior Cruciate Ligament: A Systematic Review of Imaging and Cadaveric Studies Reporting Normal Center Locations. Am J Sports Med 2017;45:2180-8. [Crossref]
21. Xu H, Zhang C, Zhang Q, Du T, Ding M, Wang Y, Fu SC, Hopkins C, Yung SH. A Systematic Review of Anterior Cruciate Ligament Femoral Footprint Location Evaluated by Quadrant Method for Single-Bundle and Double-Bundle Anatomic Reconstruction. Arthroscopy 2016;32:1724-34. [Crossref]